Available online at www.sciencedirect.com
SCIENCE DIRECT
Biochimica et Biophysica Acta 1758 (2006) 241–247
BIOCHIMICA ET BIOPHYSICA ACTA
BBA
http://www.elsevier.com/locate/bba

Hydrodynamic properties of porcine bestrophin-1 in Triton X-100

J. Brett Stanton [a], Andrew F.X. Goldberg [e], George Hoppe [f], Lihua Y. Marmorstein [a,c,d], Alan D. Marmorstein [a,b,*]

[a] Department of Ophthalmology and Vision Science, University of Arizona, Tucson, AZ 85711, USA
[b] College of Optical Sciences, University of Arizona, Tucson, AZ 85724, USA
[c] Department of Physiology, University of Arizona, Tucson, AZ 85724, USA
[d] Department of Cell Biology and Anatomy, University of Arizona, Tucson, AZ 85724, USA
[e] Eye Research Institute, Oakland University, Rochester, MI, 48309, USA
[f] Cole Eye Institute, Cleveland Clinic Foundation, Cleveland, OH 44195, USA

Received 19 December 2005; received in revised form 24 January 2006; accepted 27 January 2006
Available online 6 March 2006

Abstract

Bestrophin-1 (Best-1) is an integral membrane protein, defects in which cause Best vitelliform macular dystrophy. Best-1 is proposed to function as a Cl^- channel and/or a regulator of Ca^{++} channels. A tetrameric (or pentameric) stoichiometry has been reported for recombinant best-1. Using a combination of gel exclusion chromatography and velocity sedimentation we examined the quaternary structure of native best-1 and found that it migrates as a single species with a Stokes radius of 7.3 nm, sedimentation coefficient ($S_{20,w}$) of 4.9, and partial specific volume (v) of 0.80 ml/g. The mass of the protein–detergent complex is calculated to be 206 kDa, with the protein component estimated to be ~138 kDa. Given a monomeric mass of 68 kDa, we conclude that native best-1 solubilized with Triton X-100 is a homodimer. The differences between this observation and a prior report were examined by comparing recombinant best-1 with tissue derived best-1 using gel exclusion chromatography. Much of the recombinant best-1 eluted in the column void (V_o) fraction, unlike that extracted from RPE cells. We conclude that the minimal functional unit of best-1 is dimeric. This stoichiometry differs from that previously measured for recombinant best-1, suggesting that further studies are necessary to determine the stoichiometry of functional best-1 in RPE membranes.

Keywords: Ion channel; Calcium; Chloride; Oligomer; Centrifugation; Gel exclusion chromatography

1. Introduction

Best-1 is the prototypic member of the bestrophin or RFP-TM family of proteins [1]. There are 4 bestrophins in the human genome. Best-1 is a protein of 68 kDa, is found in the basolateral plasma membrane of retinal pigment epithelial (RPE) cells [2], and is encoded by the *VMD2* gene. Mutations in *VMD2* have been reported to cause Best vitelliform macular dystrophy (BMD) [3,4], autosomal dominant vitreoretinalchoroiditis (ADVIRC, [5]) and adult onset vitelliform macular dystrophy (AVMD, [6–10]. BMD is characterized by early onset degeneration of the macula [11], a specialized region of the retina with the fovea at its center. Both BMD and AVMD are clinically characterized by an egg yolk-like vitelliform lesion in the ocular fundus [12,13]. The hallmark of BMD is the finding of an abnormal light peak (LP) recorded via electrooculography (EOG), without aberrations in the a- or b-waves of the clinical electroretinogram (ERG) [14]. This is the diagnostic criterion that separates Best disease from AVMD. Despite this, at least two mutations in *VMD2* have been reported to cause both BMD and AVMD [15]. EOG abnormalities have also been reported in patients with ADVIRC, though typically these are also accompanied by a subnormal clinical ERG response [16]. The EOG LP can be monitored more precisely using DC amplification of the ERG [17]. DC-ERG studies on chick retina/RPE/choroid preparations have shown that the LP is generated by a depolarization of the basolateral plasma membrane of the RPE due to activation of a Cl^- conductance [18,19].

* Corresponding author. Department of Ophthalmology, University of Arizona, 655 N. Alvernon Way, Suite 108, Tucson, AZ 85711, USA. Tel.: +1 520 626 0449; fax: +1 520 626 0457.
E-mail address: amarmorstein@eyes.arizona.edu (A.D. Marmorstein).

0005-2736/$ - see front matter © 2006 Elsevier B.V. All rights reserved.
doi:10.1016/j.bbamem.2006.01.024

Based on the phenotype of BMD and the basolateral plasma membrane localization of best-1 [2], Sun et al. [20] hypothesized that bestrophin functions as a Ca^{++} dependent Cl^{-} channel and that it directly generates the LP. These data are supported by whole cell patch clamp studies of bestrophins heterologously overexpressed in cultured cells [20,21] combined with the finding that best-1 expressed in HEK293 cells forms homo-tetramers [20], a structure consistent with a pore-forming protein. Recently, we have shown that best-1 can also modify the kinetics of voltage-dependent Ca^{++} channels [22] in RPE cells.

Here, we sought to determine the hydrodynamic properties and molecular mass of the endogenous best-1 complex from RPE cells. We find that the minimal unit of the best-1 complex is a homodimer and that overexpression of recombinant best-1 in cell culture leads to the formation of protein aggregates which are not present in RPE cells in situ. Given the difference between the current findings and a previous investigation that reported a tetrameric stoichiometry, [20,23–26], we conclude that further investigations will be required to conclusively determine the stoichiometry of the best-1 functional unit in RPE membranes.

2. Materials and methods

2.1. Immunoprecipitation of best-1

Various porcine tissues and organs were obtained from a slaughterhouse (Hatfield Quality Meats, Hatfield, PA). Tissues were homogenized in a lysis buffer containing 1.0% Triton X-100 in 50 mM Tris, pH 8.0, 150 mM NaCl, 0.5 mM EDTA, protease inhibitor cocktail III (Calbiochem, San Diego, CA). After centrifugation at 10,000×*g* at 4 °C for 30 min to remove debris, the protein concentration of the lysates was determined using a BCA assay (Pierce). Best-1 was immunoprecipitated from quantities of lysate containing 1 g of total protein using rabbit polyclonal anti-bestrophin antibody [Pab-125, [2]] as before [27]. Immunoprecipitates were resuspended in SDS-PAGE sample buffer, heated for 5 min at 95 °C and resolved by SDS-PAGE. After transfer to PVDF membranes, best-1 was detected by Western blot using monoclonal antibody E6-6.

2.2. Cell culture and transfections

HEK 293 cells were maintained in a 95% air 5%/CO_2 environment at 37 °C. Cells plated at 60–80% confluency were transfected with wild type best-1 contained within the pAdlox plasmid using lipofectamine. Cells were harvested by scraping into 1 ml of Ca^{++}- and Mg^{++}-free phosphate-buffered saline 48 h after transfection.

2.3. Immunofluorescence microscopy

HEK 293 cells grown on glass coverslips were transfected with the plasmid pAdlox-kBest using lipofectamine. After 24–48 h, cells were washed with PBS and placed for 10 min in ice cold methanol. Cells were stained for best-1 using monoclonal antibody E6-6 as described previously [2] with a FITC coupled goat anti-mouse IgG secondary antibody. Coverslips were mounted in fluormount and cells were examined using a Nikon E-600 fluorescence microscope. Images were acquired with a cooled CCD camera and ACTII software (Nikon).

2.4. Isolation of RPE cells and sample preparation

RPE cells were harvested from porcine eyes in phosphate buffered saline (PBS) as described previously [2]. Cell pellets were stored at −80 °C until use. For gel exclusion chromatography experiments, RPE cells were further fractionated using a modification of the procedure of West et al. [28]. In brief, RPE from >50 porcine eyes were resuspended in 2 ml of 10 mM HEPES, 150 mM KCl, 2 mM $CaCl_2$, 0.25 M sucrose, 100 μM phenylmethylsulfonyl-fluoride, and 0.1% (v/v) protease inhibitor cocktail III (Calbiochem, San Diego, CA) and were homogenized using a Dounce homogenizer. The homogenate was centrifuged at 5000×*g* for 10 min at 4 °C to remove intact cells and nuclei. The supernatant was then centrifuged at 60,000×*g* for 90 min at 4 °C and the pellet, which contained the majority of best-1, was harvested and stored at −80 °C.

2.5. Gel exclusion chromatography

Measurement of the Stokes radius of best-1 was performed using porcine RPE membranes (enriched as described above), or whole cell lysates derived from porcine RPE, or transfected HEK 293 cells. Membranes were solubilized in 1% Triton X-100 in 10 mM HEPES, pH 7.4, 150 mM KCl, 2 mM $CaCl_2$, and soluble extracts were loaded onto columns (1.6×60 cm) of either Sephacryl S-300HR or Sephacryl S-400HR (Amersham) that were equilibrated with 0.2% Triton X-100 in 10 mM HEPES, pH 7.4, 150 mM KCl, 2 mM $CaCl_2$. The column was developed at a linear flow rate of 30 ml cm^{-1} h^{-2}., and 1 ml fractions were collected. Best-1 was immunoprecipitated from fractions using Pab-125 as described previously [2] and was detected by SDS-PAGE and Western blotting with monoclonal antibody E6-6. Columns were calibrated using individually chromatographed standards (thyroglobulin, ferritin, cytosine, catalase, aldolase, albumin, and RNase A) with known Stokes radius . The void volume (V_o) was determined for the Sephacryl S300-HR column using Blue Dextran and for the Sephacryl S-400HR column using plasmid DNA (pBluescript). The total column volume (V_t) was determined using cytosine. The Stokes radius of best-1 was determined according to the method of Laurent and Killander [29] from the position of the major best-1 peak in 4 separate runs of the Sephacryl S-300HR column and verified in subsequent experiments using the Sephacryl S-400HR column.

2.6. Sucrose density gradient sedimentation

The sedimentation coefficient ($S_{20,w}$) and partial specific volume (v) of best-1 was determined according to the method of Clarke and Smigel [30], assuming that equal amounts of detergent are bound in H_2O and D_2O. Linear gradients of 5–20% (w/v) sucrose were prepared in H_20 or 92% D_2O containing 0.2% (v/v) Triton X-100, 10 mM HEPES, pH 7.4, 150 mM KCl, and 2 mM $CaCl_2$ using a Gradient Master 107 (BioComp, Fredericton, New Brunswick, CAN). Samples (500 μl) containing marker enzymes [1 mg/ml of lysozyme (2.1 S, [31]), aldolase (7.7 S, [32]), catalase (11.3 S, [33]), and β-galactosidase (15.9 S, [34]] were loaded onto gradients of 12.5 ml final volume and centrifuged in a Sorval TH-641 rotor at 39,000 RPM at 4 °C for 16 h (H_2O gradients) or 30 h (D_2O gradients). After centrifugation, tubes were punctured at their base and 0.5 ml fractions were collected drop wise. Fractions were assayed for marker enzymes as described in the Worthington Enzyme Manual. The fractions were analyzed for best-1 by SDS-PAGE and Western blotting with monoclonal antibody E6-6 as described previously [2]. Blots were scanned and the position of best-1 in the gradient determined by densitometric analysis using Metamorph, ver. 4.6 (Molecular Devices).

2.7. Estimation of molecular mass and stoichiometry of the best-1/detergent complex

Calculation of the molecular mass of the best-1/detergent complex was made after measurement of the Stokes radius, $S_{20,w}$, and v, and application of the Svedberg equation as described by Clarke and Smigel [30]. Estimation of the protein portion of the complex was performed assuming additivity of v for Triton X-100 (0.94 ml/g) and protein (0.74 ml/g), and calculated according to Clarke [35]. Stoichiometry was determined based on the molecular mass of the protein portion of the best-1–detergent complex and the molecular mass of monomeric best-1 as determined by SDS-PAGE [2,36] following the assumption that best-1 constitutes 100% of the protein in the complex.

3. Results

The characterization of membrane protein structure is technically challenging; defining the stoichiometry of best-1

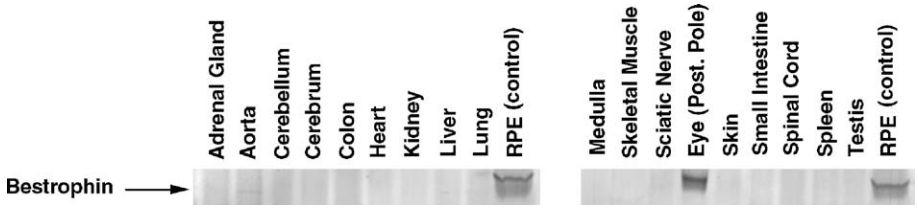

Fig. 1. Expression of best-1 in porcine tissues. Best-1 was immunoprecipitated from lysates of various porcine tissues/organs containing 1 g of total protein using a polyclonal anti-best-1 antibody. Immunoprecipitates were resolved by SDS-PAGE transferred to PVDF and probed with a monoclonal anti-best-1 antibody. Lanes containing porcine RPE were used as controls. Best-1 was found only in lysates from the posterior pole of the eye and not in any other tissue or organ.

is made more difficult considering the low abundance of best-1 and of RPE cells in a single animal. A previous study avoided the latter constraint by using metabolic labeling of recombinant best-1 in cultured 293 cells [20]. That investigation measured a tetra- or pentameric stoichiometry, a finding consistent with the notion that this molecule acts as an ion channel. We wished to examine whether native best-1 from RPE cells adopts a similar quaternary structure, and choose the method of Clarke and Smigel [30], as applied by Goldberg and Molday [32]. This method, by taking advantage of hydrodynamic analysis and the sensitivity of Western blot detection, allows for the determination of molecular mass (and thereby stoichiometry), of a low-concentration and unpurified target protein. It requires knowledge of the Stokes radius, sedimentation coefficient ($S_{20,w}$), detergent binding, and partial specific volume (v) of the detergent–protein complex.

Best-1 mRNA has been identified in RPE, testis, and brain by reverse transcription PCR [3,4]. Since a large amount of best-1 would be required for our studies, we required an abundant source of best-1. Our antibodies have been shown to react with human, monkey, and pig best-1 [2]. Of these species, porcine tissues are the easiest to obtain in large quantities. We next examined the abundance of best-1 in porcine tissues. Tissues were homogenized in a lysis buffer containing 1% Triton X-100. For each organ or tissue, best-1 was immunoprecipitated from a volume of lysate containing 1 g of total protein. As shown in Fig. 1, best-1 was detected only in the posterior pole of the eye. We have previously shown that best-1 is expressed uniquely in the RPE in the eye [2]. Therefore, we conclude that the RPE is the sole source of best-1.

To determine the Stokes radius of best-1, RPE cells collected from porcine eyes were lysed in a buffer containing 1% Triton X-100. The lysate was applied to a Sephacryl S-300HR column that had been pre-calibrated with protein standards of known Stokes radius. Best-1 was detected in column fractions by immunoprecipitation followed by Western blot (Fig. 2A). Four

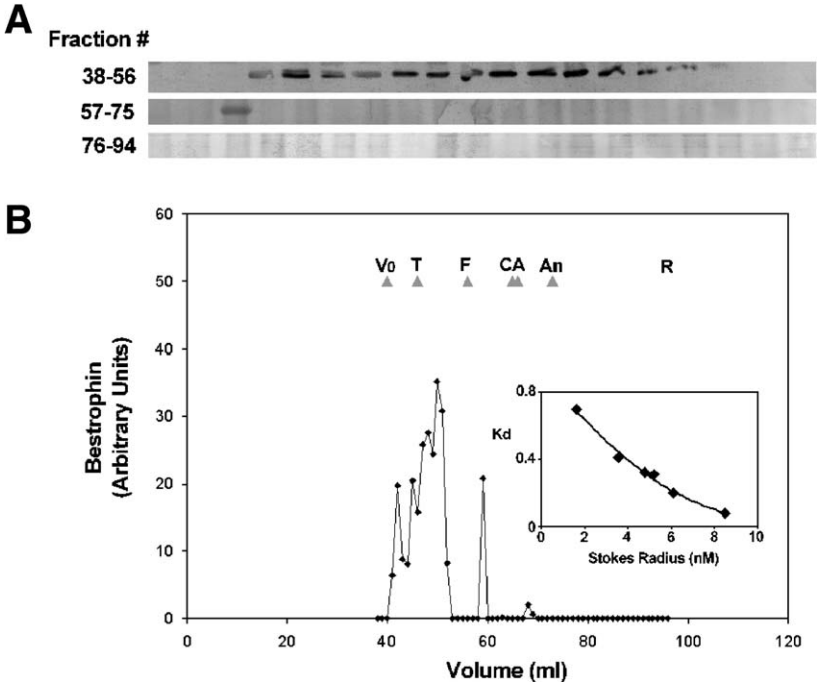

Fig. 2. Gel exclusion chromatography of best-1 complexes. Porcine RPE lysates were resolved by gel filtration chromatography using Sephacryl-S300HR. 1 ml fractions were collected and the presence of best-1 determined by immunoprecipitation followed by immunoblotting (A) with anti-best-1 antibodies. Densitometric analysis of band intensities (B) indicates that best-1 exists predominantly as a single peak with a Stokes radius of ~7.3 nm. A single band eluting in fraction 59 was present in all experiments and most likely represents a small amount of best-1 monomer. Panels shown are representative of 4 independent experiments. V_o=Void, T=thyroglobulin, F=ferritin, C=catalase, A=aldolase, An=albumin, R=RNase A.

independent runs were performed. Best-1 eluted as one major species with a peak occurring between the thyroglobulin (8.5 nm) and ferritin (6.1 nm) standards. From the standard curve (Fig 1b inset) the Stokes radius of detergent–best-1 complexes was determined to be ~7.3 nm.

To determine the sedimentation coefficient ($S_{20,w}$), detergent binding, and partial specific volume (v) of best-1, velocity sedimentation of RPE lysates was performed in 5%–20% sucrose gradients containing 0.2% Triton X-100- formed using either H_2O ($n=8$, Fig. 3) or D_2O ($n=8$, Fig. 4). Based on the position of best-1 in the gradients as determined by Western blotting, $S_{20,w}$ was calculated to be 4.9 ± 0.4, $v=0.80\pm0.02$ ml/g, and detergent to constitute 31% of the complex or 0.48 ± 0.24 g Tx-100/g protein. These values together with the Stokes radius were applied to the Svedberg equation as modified by Clarke [35] to determine the mass of the detergent–best-1 complex. That value was found to be ~206 kDa. Adjusting for the amount of Triton X-100 bound to the complex, the mass of protein in the detergent–best-1 complex was calculated to be ~138 kDa. Best-1 has a monomeric mass of 68 kDa based on its primary amino acid sequence and SDS-PAGE [2,36]. Assuming the complex is comprised exclusively of best-1, a finding consistent with our prior work and the findings of others [20,36], we find that native best-1 exists as stable dimers in Triton X-100 solution.

These findings were surprising, given a previous investigation by Sun et al. [20] that reported a tetrameric (or pentameric) stoichiometry for recombinant best-1 expressed in HEK 293 cells. We hypothesized that differences in expression system might account, at least in part, for the observed discrepancy in quaternary structure and used size exclusion chromatography to compare the behavior of recombinant best-1 with that from porcine RPE cells.

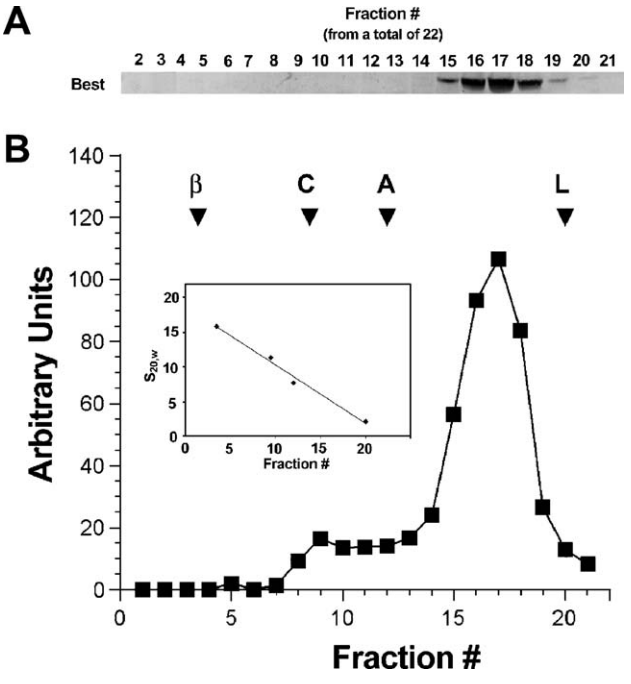

Fig. 3. Velocity sedimentation analysis of best-1 in H_2O. Lysates of porcine RPE cells were sedimented through a continuous 5–20% sucrose gradient prepared in H_2O as described in Materials and methods. Fractions were collected and best-1 detected by Western blot (A). The position of best-1 in the gradient was determined from densitometric plots of the immunoblots (B). Panels shown are representative of 8 separate experiments. β = β-galactosidase; C = catalase, A = aldolase, L = lysozyme.

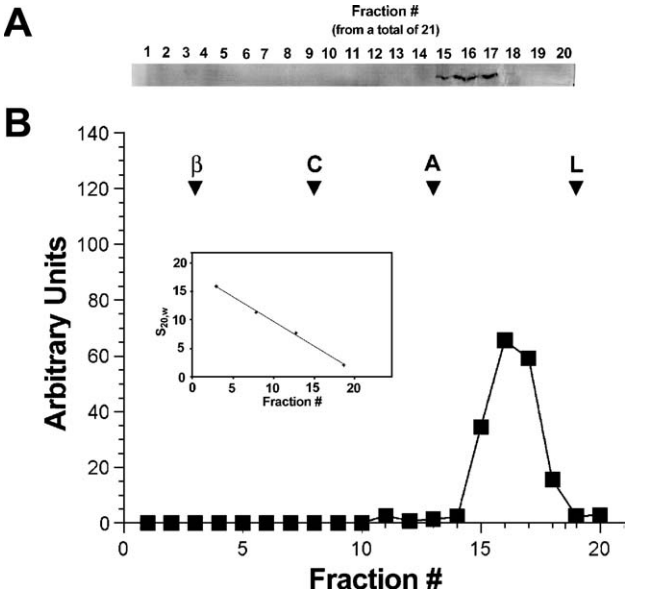

Fig. 4. Velocity sedimentation analysis of best-1 in D_2O. Lysates of porcine RPE cells were sedimented through a continuous 5–20% sucrose gradient prepared in D_2O as described in Materials and methods. Fractions were collected and best-1 detected by Western blot (A). The position of best-1 in the gradient was determined from densitometric plots of the immunoblots (B). Panels shown are representative of 5 separate experiments. β = β-galactosidase; C = catalase, A = aldolase, L = lysozyme.

To determine whether recombinant best-1 exhibits hydrodynamic properties similar to those of best-1 from RPE cells, we analyzed the Stokes radius of each molecule using gel exclusion chromatography on Sephacryl S-400 (Fig. 6). Sephacryl S-400 was used in these experiments in order to increase resolution of complexes with Stokes radii greater than 7.3 nm. As was determined using Sephacryl S-300, in 0.2% Triton X-100, best-1 complexes exhibit a Stokes radius of 7.3 nm. Best-1 complexes solubilized from porcine RPE migrated with mobility reflecting a Stokes radius of 7.3 nm, similar to that measured previously (Fig. 2). In contrast, in lysates of transfected HEK 293 cells, best-1 eluted in a markedly different fashion, exhibiting peak broadening, a shift to earlier elution time, and heterogeneity (Fig. 6). The bimodal distribution likely reflects at least two distinct populations, with the material eluting in the column void volume representing highly aggregated best-1. There is also a small shift in the main peak, suggesting that a greater fraction of the best-1 is present in larger complexes. This shift and significant peak broadening might reflect partially unfolded protein or differences in post-translation modification(s). Overall these results indicate that a significant fraction (>36%) of the best-1 solubilized from HEK 293 cells exhibits a substantially different hydrodynamic character than that solubilized from native RPE cells.

The observation that a major fraction of best-1 solubilized from HEK 293 cells elutes with larger Stokes radii

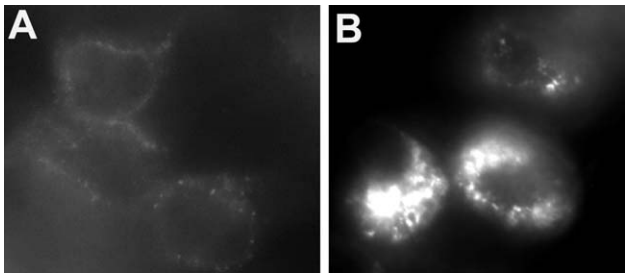

Fig. 5. Immunofluorescence localization of best-1 in transfected HEK 293 cells. HEK 293 cells were transfected with pAdlox-Best and stained for best-1 using a monoclonal antibody against best-1 and a texas red labeled secondary antibody. 2 populations of cells were observed. Lightly stained cells (A) exhibited a circumferential pattern of punctate staining consistent with a plasma membrane localization. Brighter cells exhibited large intracellular perinuclear aggregates of best-1 (B).

prompted us to examine the subcellular distribution of recombinant best-1 in these cells. Fluorescence images of HEK 293 cells expressing a best-1–EGFP fusion protein are presented in Fig. 5. The transfected cell population showed a heterogenous level of protein expression. Modestly expressing cells exhibited a pattern of staining most consistent with plasma membrane and endocytic localization (Fig. 5A). More highly expressing cells displayed focal intracellular accumulations of best-1–GFP (Fig 5B); a pattern typical of protein misfolding and aggregation. These findings are consistent with the SEC characterization of HEK 293 expressed best-1, and suggest that a significant fraction of this protein may be misfolded.

4. Discussion

Explaining the pathogenic effects of mutations in *VMD2* and the development of Best vitelliform macular dystrophy (BMD) will require an improved understanding of the structure and function of the *VMD2* gene product, best-1. BMD is characterized, in part, by an abnormal EOG LP [14]. Since activation of a basolateral Cl^- conductance appears to underlie the normal LP [18,19], it seems reasonable to expect that BMD-associated mutations directly or indirectly affect a Cl^- conductance situated in the basolateral RPE membrane. Several studies have presented evidence that best-1 functions directly as a Ca^{++}-activated chloride channel; however, all are based on analyses using heterologously expressed proteins (reviewed in [21]). In contrast, recent data derived from expression studies using an RPE cell line suggest that best-1 acts as a voltage-dependent Ca^{++} channel regulator [37]. In support of this hypothesis, studies using overexpression of human best-1 in rats [38] suggest that best-1 functions to modulate Cl^- conductance in RPE basolateral membranes. Overexpression caused a desensitization of light responses—suggesting an indirect, rather than a direct role for best-1 in generating the RPE Cl^- conductance. Best-1 molecular function is currently being debated [39], and knockout and transgenic mouse models

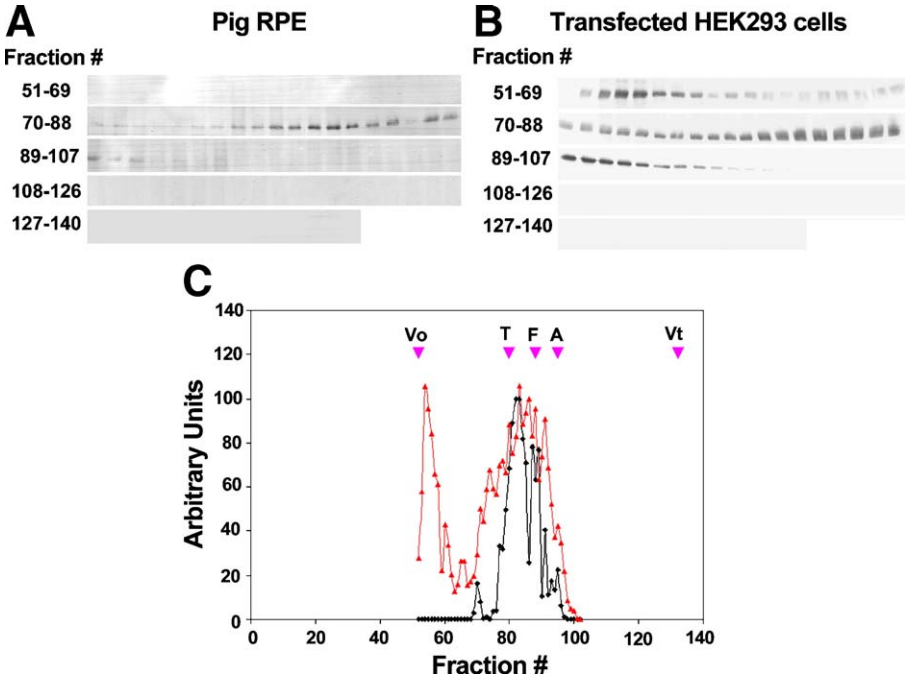

Fig. 6. Gel exclusion chromatography of recombinant vs. native best-1 on Sephacryl S-400HR. The elution profile of native best-1 protein in porcine RPE lysates (A) was compared to that of recombinant best-1 in lysates of transfected HEK 293 cells (B). Following chromatography over a Sephacryl S-400HR column, best-1 was immunoprecipitated from fractions and subject to Western blotting with a second anti-best-1 antibody. Inspection of densitometric plots of best-1 indicated that best-1 in native RPE eluted predominantly as a single species with a Stokes radius of ~7.3 nm (C, black), consistent with our observations using Spephacryl S-300HR (see Fig. 1). A similar analysis of recombinant best-1 resulted in the identification of 2 primary peaks of best-1 immunoreactivity (C, red). The first peak eluted in the column V_o and was not observed in native RPE. The second peak eluted at the same position as the best-1 peak observed in native RPE. However, this peak was broader than that observed in lysates of native RPE. Data are representative of 3 independent experiments. V_o = Void, T = Thyroglobulin, F = ferritin, A = aldolase, V_t = included volume of the column determined using cytosine.

should help to clarify the physiological function of normal best-1 and the role that best-1 defects play in BMD.

The current study aimed to determine the stoichiometry of best-1 from an endogenous source. A screen of best-1 expression in porcine tissues (Fig. 1) found significant best-1 levels only in RPE. Therefore, our analyses were performed on best-1 in Triton X-100 extracts of porcine RPE. Stoichiometry was determined by estimating the molecular mass of detergent solubilized best-1 using the method of Clarke and Smigel [30]. This approach combines several hydrodynamic measures to derive molecular mass for a detergent-solubilized low abundance integral membrane protein in a complex mixture; it assumes that the species of interest is not interacting with other components. Although in a previous study, we identified protein phosphatase 2A as capable of physically and functionally interacting with best-1 [27], that association was documented to be weak and sub-stoichiometric.

Using gel exclusion chromatography and velocity sedimentation, we determined the hydrodynamic properties of best-1. Based on these measurements, we have estimated a molecular mass of 138 kDa for the detergent-free best-1 complex. Given that *VMD2* encodes a 68 kDa protein, the predicted mass of a best-1 homodimer is 136 kDa. Therefore, our data suggests that best-1 forms stable homodimers when solubilized in Triton X-100. We cannot however exclude the possibility that these complexes represent a heterodimer of best-1 and best-2. Prior studies using RT-PCR have suggested that best-2 is expressed by the RPE [40]. If sized similarly to its human ortholog, the porcine best-2 splice variant would be predicted to have a monomeric mass of ~57 kDa. Since the hydrodynamic analysis used is insufficient to resolve best-1 homodimers (~136 kDa) from best-1/best-2 heterodimers (~125 kDa), future studies will be required to address this possibility. Regardless, the results obtained here indicate that the minimal unit of best-1 function is a dimer.

This finding is consistent with the previously proposed notion that best-1 functions as an oligomer, but differs in absolute stoichiometry, as determined in HEK 293 cells [41]. That study found a tetrameric (or pentameric) subunit stoichiometry, suggested to reflect best-1 function as a Cl^- channel. Our finding that best-1 is extracted from RPE membranes in a dimeric form does not preclude the possibility that Triton X-100 solubilization disrupts a higher-order structure present in RPE membranes; however, we are not aware of precedents for this type of behavior amongst eukaryotic ion selective channels. We have shown that a large fraction of best-1 in transfected HEK 293 cells is present as higher order aggregates that are not present in native RPE cells. It is possible that the tetrameric (or pentameric) stoichiometry measured for recombinant best-1 also reflects a non-native property. Determination of membrane protein stoichiometry in situ is a difficult proposition, as evidenced by long-running debates for proteins as plentiful as rhodopsin [42,43]. Our findings illustrate the utility of comparing biochemical data obtained from recombinant proteins expressed in a heterologous system to the native protein derived from its tissue source, and suggest that additional study will be required to determine the stoichiometry of the best-1 functional unit in RPE membranes.

In summary, here we demonstrate that native best-1 solubilized in Triton X-100 forms dimers rather than the homo-tetramers predicted based on examination of recombinant protein overexpressed in a heterologous cell culture system. The difference in stoichiometry may result from the formation of aggregates of best-1 in transfected cells and/or differences in the behavior of membrane-bound vs. detergent solubilized protein. The hypothesis that best-1 functions as a calcium-activated Cl^- channel in the RPE is in part based on the proposed tetrameric structure of the protein. Our recent findings in *Vmd2* deficient mice (our unpublished observations), and the finding that best-1 alters the kinetics of voltage dependent Ca^{++} channels [22] suggest that best-1 may be capable of functions other than or in addition to Cl^- ion transport. Further studies are necessary to better understand the structure of best-1 and how that structure facilitates the functions of the protein.

Acknowledgements

Work in the author's laboratories is funded by NIH grants EY13160 and EY14898 to ADM, EY13847 to LYM, funds from Phillip Morris USA and Phillip Morris International, and the Macular Degeneration Foundation to ADM, a Career Development Award from Research to Prevent blindness to LYM, and an unrestricted grant from Research to Prevent Blindness to the Department of Ophthalmology at the University of Arizona.

References

[1] H. Stohr, A. Marquardt, I. Nanda, M. Schmid, B.H. Weber, Three novel human VMD2-like genes are members of the evolutionary highly conserved RFP-TM family, Eur. J. Hum. Genet. 10 (2002) 281–284.

[2] A.D. Marmorstein, L.Y. Marmorstein, M. Rayborn, X. Wang, J.G. Hollyfield, K. Petrukhin, Bestrophin, the product of the Best vitelliform macular dystrophy gene (VMD2), localizes to the basolateral plasma membrane of the retinal pigment epithelium, Proc. Natl. Acad. Sci. U. S. A. 97 (2000) 12758–12763.

[3] K. Petrukhin, M.J. Koisti, B. Bakall, W. Li, G. Xie, T. Marknell, O. Sandgren, K. Forsman, G. Holmgren, S. Andreasson, M. Vujic, A.A. Bergen, V. McGarty-Dugan, D. Figueroa, C.P. Austin, M.L. Metzker, C.T. Caskey, C. Wadelius, Identification of the gene responsible for Best macular dystrophy, Nat. Genet. 19 (1998) 241–247.

[4] A. Marquardt, H. Stohr, L.A. Passmore, F. Kramer, A. Rivera, B.H. Weber, Mutations in a novel gene, VMD2, encoding a protein of unknown properties cause juvenile-onset vitelliform macular dystrophy (Best's disease), Hum. Mol. Genet. 7 (1998) 1517–1525.

[5] J. Yardley, B.P. Leroy, N. Hart-Holden, B.A. Lafaut, B. Loeys, L.M. Messiaen, R. Perveen, M.A. Reddy, S.S. Bhattacharya, E. Traboulsi, D. Baralle, J.J. De Laey, B. Puech, P. Kestelyn, A.T. Moore, F.D. Manson, G.C. Black, Mutations of VMD2 splicing regulators cause nanophthalmos and autosomal dominant vitreoretinochoroidopathy (ADVIRC), Invest. Ophthalmol. Vis. Sci. 45 (2004) 3683–3689.

[6] R. Allikmets, J.M. Seddon, P.S. Bernstein, A. Hutchinson, A. Atkinson, S. Sharma, B. Gerrard, W. Li, M.L. Metzker, C. Wadelius, C.T. Caskey, M. Dean, K. Petrukhin, Evaluation of the Best disease gene in patients with age-related macular degeneration and other maculopathies, Hum. Genet. 104 (1999) 449–453.

[7] B. Bakall, T. Marknell, S. Ingvast, M.J. Koisti, O. Sandgren, W. Li,

A.A. Bergen, S. Andreasson, T. Rosenberg, K. Petrukhin, C. Wadelius, The mutation spectrum of the bestrophin protein-functional implications, Hum. Genet. 104 (1999) 383–389.
[8] F. Kramer, N. Mohr, U. Kellner, G. Rudolph, B.H. Weber, Ten novel mutations in VMD2 associated with Best macular dystrophy (BMD), Hum. Mutat. 22 (2003) 418.
[9] J.M. Seddon, M.A. Afshari, S. Sharma, P.S. Bernstein, S. Chong, A. Hutchinson, K. Petrukhin, R. Allikmets, Assessment of mutations in the Best macular dystrophy (VMD2) gene in patients with adult-onset foveomacular vitelliform dystrophy, age-related maculopathy, and bull's-eye maculopathy, Ophthalmology 108 (2001) 2060–2067.
[10] K. White, A. Marquardt, B.H. Weber, VMD2 mutations in vitelliform macular dystrophy (Best disease) and other maculopathies, Hum. Mutat. 15 (2000) 301–308.
[11] V. Godel, G. Chaine, L. Regenbogen, G. Coscas, Best's vitelliform macular dystrophy, Acta Ophthalmol., Suppl. 175 (1986) 1–31.
[12] M.F. Marmor, K. Small, in: M.F. Marmor, T. Wolfensberger (Eds.), The Retinal Pigment Epithelium, Oxford Press, New York, 1998, pp. 330–333.
[13] D.J.M. Gass, in: D.J.M. Gass (Ed.), Stereoscopic Atlas of Macular Diseases, Diagnosis and Treatment, Mosby, St. Louis, 1997, pp. 303–313.
[14] H.E. Cross, L. Bard, Electro-oculography in Best's muscular dystrophy, Am. J. Ophthalmol. 77 (1974) 46–50.
[15] F. Kramer, K. White, D. Pauleikhoff, A. Gehrig, L. Passmore, A. Rivera, G. Rudolph, U. Kellner, M. Andrassi, B. Lorenz, K. Rohrschneider, A. Blankenagel, B. Jurklies, H. Schilling, F. Schutt, F.G. Holz, B.H. Weber, Mutations in the VMD2 gene are associated with juvenile-onset vitelliform macular dystrophy (Best disease) and adult vitelliform macular dystrophy but not age-related macular degeneration, Eur. J. Hum. Genet. 8 (2000) 286–292.
[16] D.P. Han, M.F. Lewandowski, Electro-oculography in autosomal dominant vitreoretinochoroidopathy, Arch. Ophthalmol. 110 (1992) 1563–1567.
[17] R.H. Steinberg, R.A. Linsenmeier, E.R. Griff, in: N.N. Osborne, G.J. Chader (Eds.), Progress in Retinal Research, Pergamon Press, Oxford, 1985, pp. 33–66.
[18] R.P. Gallemore, R.H. Steinberg, Effects of DIDS on the chick retinal pigment epithelium: II. Mechanism of the light peak and other responses originating at the basal membrane, J. Neurosci. 9 (1989) 1977–1984.
[19] R.P. Gallemore, R.H. Steinberg, Light-evoked modulation of basolateral membrane Cl-conductance in chick retinal pigment epithelium: the light peak and fast oscillation, J. Neurophysiol. 70 (1993) 1669–1680.
[20] H. Sun, T. Tsunenari, K.W. Yau, J. Nathans, The vitelliform macular dystrophy protein defines a new family of chloride channels, Proc. Natl. Acad. Sci. U. S. A. 99 (2002) 4008–4013.
[21] C. Hartzell, I. Putzier, J. Arreola, Calcium-activated chloride channels, Annu. Rev. Physiol. 67 (2005) 719–758.
[22] R. Rosenthal, B. Bakall, T. Kinnick, N. Peachey, S. Wimmers, C. Wadelius, A. Marmorstein, O. Strauss, Expression of bestrophin-1, the product of the VMD2 gene, modulates voltage-dependent Ca2+ channels in retinal pigment epithelial cells. FASEB J. in press.
[23] Z. Qu, C. Hartzell, Determinants of anion permeation in the second transmembrane domain of the mouse bestrophin-2 chloride channel, J. Gen. Physiol. 124 (2004) 371–382.
[24] Z. Qu, R. Fischmeister, C. Hartzell, Mouse bestrophin-2 is a bona fide Cl(−) channel: identification of a residue important in anion binding and conduction, J. Gen. Physiol. 123 (2004) 327–340.
[25] T. Tsunenari, H. Sun, J. Williams, H. Cahill, P. Smallwood, K.W. Yau, J. Nathans, Structure–function analysis of the bestrophin family of anion channels, J. Biol. Chem. 278 (2003) 41114–41125.
[26] Z. Qu, R.W. Wei, W. Mann, H.C. Hartzell, Two bestrophins cloned from *Xenopus laevis* oocytes express Ca(2+)-activated Cl(−) currents, J. Biol. Chem. 278 (2003) 49563–49572.
[27] L.Y. Marmorstein, P.J. McLaughlin, J.B. Stanton, L. Yan, J.W. Crabb, A.D. Marmorstein, Bestrophin interacts physically and functionally with protein phosphatase 2A, J. Biol. Chem. 277 (2002) 30591–30597.
[28] K.A. West, L. Yan, K. Shadrach, J. Sun, A. Hasan, M. Miyagi, J.S. Crabb, J.G. Hollyfield, A.D. Marmorstein, J.W. Crabb, Protein database, human retinal pigment epithelium, Mol, Cell Proteomics 2 (2003) 37–49.
[29] T.C. Laurent, J. Killander, J. Chromatogr. 14 (1964) 317–330.
[30] S. Clarke, M.D. Smigel, Size and shape of membrane protein-detergent complexes: hydrodynamic studies, Methods Enzymol. 172 (1989) 696–709.
[31] R.G. Martin, B.N. Ames, A method for determining the sedimentation behavior of enzymes: application to protein mixtures, J. Biol. Chem. 236 (1961).
[32] A.F.X. Goldberg, R.S. Molday, Subunit composition of the peripherin/rds-rom-1 disk rim complex from rod photoreceptors: hydrodynamic evidence for a tetrameric quaternary structure. Biochemistry 35 (1996) 6144–6149.
[33] J.B. Sumner, N. Gralén, The molecular weight of crystalline catalase, J. Biol. Chem. 125 (1938) 33–36.
[34] R.A. Aiyer, Structural characterization of insulin receptors. I. Hydrodynamic properties of receptors from turkey erythrocytes. J. Biol. Chem. 258 (1983) 14992–14999.
[35] S. Clarke, The size and detergent binding of membrane proteins, J. Biol. Chem. 250 (1975) 5459–5469.
[36] L.Y. Marmorstein, P.J. McLaughlin, J.B. Stanton, L. Yan, J.W. Crabb, A.D. Marmorstein, Bestrophin interacts physically and functionally with protein phosphatase 2A, J. Biol. Chem. 277 (2002) 30591–30597.
[37] R. Rosenthal, B. Bakall, T. Kinnick, N. Peachey, S. Wimmers, C. Wadelius, A. Marmorstein, O. Strauss, Expression of bestrophin-1, the product of the VMD2 gene, modulates voltage-dependent Ca2+ channels in retinal pigment epithelial cells, FASEB J. 20 (2006) 178–180.
[38] A.D. Marmorstein, J.B. Stanton, J. Yocom, B. Bakall, M.T. Schiavone, C. Wadelius, L.Y. Marmorstein, N.S. Peachey, A model of best vitelliform macular dystrophy in rats, Invest. Ophthalmol. Vis. Sci. 45 (2004) 3733–3739.
[39] O. Strauss, R. Rosenthal, Function of bestrophin, Ophthalmologe 102 (2005) 122–126.
[40] H. Stohr, A. Marquardt, I. Nanda, M. Schmid, B.H. Weber, Three novel human VMD2-like genes are members of the evolutionary highly conserved RFP-TM family, Eur. J. Hum. Genet. 10 (2002) 281–284.
[41] H. Sun, T. Tsunenari, K.W. Yau, J. Nathans, The vitelliform macular dystrophy protein defines a new family of chloride channels, Proc. Natl. Acad. Sci. U. S. A. 99 (2002) 4008–4013.
[42] M. Chabre, M. le Maire, Monomeric G-protein-coupled receptor as a functional unit, Biochemistry 44 (2005) 9395–9403.
[43] K. Suda, S. Filipek, K. Palczewski, A. Engel, D. Fotiadis, The supramolecular structure of the GPCR rhodopsin in solution and native disc membranes, Mol. Membr. Biol. 21 (2004) 435–446.